


Deflection of light and time delay in hyperbolic Einstein-Straus–de Sitter solution

Mourad Guenouche ^{*}

*Laboratoire de Physique Théorique, Université Frères Mentouri-Constantine 1,
BP 325 route de Ain El Bey, 25017 Constantine, Algeria
and Département des Sciences de la Matière, Université Abbès Laghrour-Khenchela,
BP 1252, El Houria, Route de Constantine, 40004 Khenchela, Algeria*

(Dated: July 17, 2025)

We analyze strong gravitational lensing by a spherically symmetric mass distribution within the Einstein-Straus–de Sitter framework in a spatially open Universe with negative curvature ($k = -1$). Applying the theory to the lensed quasar SDSS J1004+4112, we identify a critical threshold for the current scale factor a_0 of approximately 2.6×10^{27} m, below which the effects of negative spatial curvature on lensing observables become significant, corresponding to a current curvature density of $|\Omega_{k0}| \gtrsim 0.0025$. In particular, for $\Omega_{k0} = -0.15$, the light bending increases slightly by $\sim 1\%$, while the time delay exhibits a more substantial increase of $\sim 10\%$. Beyond this threshold, however, the lensing observables are found to be insensitive to the current scale factor and converge to those characteristic of a spatially flat Universe. Importantly, our results indicate that, even in scenarios where spatial curvature would otherwise enhance lensing observables, the effect of the cosmological constant does remain present and acts to reduce light bending, corroborating the claim of Rindler and Ishak.

I. INTRODUCTION

Gravitational lensing provides a powerful probe of cosmic structures, but its interpretation relies critically on assumptions about the Universe’s geometry. While current cosmological observations suggest that the spatial curvature of the Universe is extremely close to zero, the possibility of a small but nonzero curvature remains open. Most gravitational lensing studies, however, assume perfect spatial flatness, allowing for the use of Euclidean geometry to estimate light deflection and time delays. Such simplifications, though convenient, break down in curved spacetimes, where photon paths deviate from straight lines even outside local inhomogeneities.

The Einstein-Straus–de Sitter (ESdS) model, with a cosmological constant Λ , is a foundational example of a Swiss-cheese cosmology [1–3], offering a self-consistent framework for studying realistic astrophysical phenomena. It elegantly reconciles cosmic expansion on large scales with local static gravitational fields by embedding a static Schwarzschild–de Sitter (SdS or Kottler) metric, which describes local systems such as galaxies or clusters, within a dynamic Friedmann–Lemaître–Robertson–Walker (FLRW) universe.

This work extends the analysis of strong gravitational lensing within the ESdS model to specifically examine the case of negative spatial curvature $k = -1$, which, despite being included in general treatments [4], remains largely underexplored in detail in the literature. Our calculations are grounded in the core principles of general relativity and are based on direct integration of null geodesic equations. This approach accommodates arbitrary spatial curvature, without recourse to flat space

approximations to compute light bending and time delay.

Motivated by ongoing debate regarding the influence of the cosmological constant Λ on light deflection [5–23], we aim to reexamine this issue in the context of a negatively curved ESdS model. While recent studies suggest that the effect is negligible, it remains an open question whether negative spatial curvature could modify or enhance this outcome. For instance, the authors of Ref [17, 24] assert that the contribution of Λ is absorbed into the impact parameter or angular diameter distance, making its direct effect minuscule. In Ref. [21], the authors find no extra measurable dependence of gravitational lensing observables on the cosmological constant beyond what is already present in the standard lensing equations within Swiss-cheese cosmological model.

The lensed quasar SDSS J1004+4112 is selected as a test case to quantify the influence of the spatial curvature and the cosmological constant on gravitational lensing observables. We assess these effects through systematic variations in the current cosmic scale factor a_0 . For direct comparison to prior analyses within flat ($k = 0$) and positively curved ($k = +1$) ESdS models, presented in Refs. [25–27], we adopt the same cosmological parameters as employed therein.

The paper is organized as follows. Section II establishes the geometric framework of the hyperbolic ESdS model by presenting the junction conditions required to match the static Schwarzschild–de Sitter vacuole to an expanding FLRW universe with negative spatial curvature. In Sec. III, the detailed methodology for computing light deflection and time delay is developed, including direct integration of null geodesic equations across the various spacetime regions leading to relevant analytical expressions. Section IV applies this formalism to the lensed quasar SDSS J1004+4112, systematically exploring how lensing observables depend on the cosmic scale

^{*} guenouche_mourad@umc.edu.dz; guenouche_mourad@univ-khenchela.dz

factor and cosmological constant, and comparing the results to those obtained in flat and closed ESdS models. Finally, Sec. V summarizes the main findings and discusses their implications for cosmological lensing, as well as possible directions for future work.

II. JUNCTION CONDITIONS FOR HYPERBOLIC EINSTEIN-STRAUS-DE SITTER METRIC

In Schwarzschild coordinates (T, r, θ, φ) , the static SdS metric

$$ds_{\text{SdS}}^2 = B(r)dT^2 - B(r)^{-1}dr^2 - r^2(d\theta^2 + \sin^2\theta d\varphi^2), \quad (1)$$

with

$$B(r) = 1 - \frac{2GM}{r} - \frac{\Lambda}{3}r^2, \quad (2)$$

applies within a vacuole (Schücking sphere) of radius $r_{\text{Schü}}(T)$ centered around a spherical mass distribution (the lens) M , $r \leq r_{\text{Schü}}$. In the Friedmann coordinates (t, r, θ, φ) , the dynamic FLRW metric, with a negative curvature constant ($k = -1$),

$$ds_{\text{FLRW}}^2 = dt^2 - a(t)^2 [d\chi^2 + \sinh^2\chi (d\theta^2 + \sin^2\theta d\varphi^2)], \quad (3)$$

describes the spacetime outside the vacuole of constant radius $\chi_{\text{Schü}}$, $\chi \geq \chi_{\text{Schü}}$, where the scale factor $a(t)$ evolves according to the Friedmann equation,

$$\frac{da}{dt} = f(a), \quad f(a) = \sqrt{\frac{A}{a} + \frac{\Lambda}{3}a^2 - k}, \quad (4)$$

with ρ the dust density and A a constant coming from the energy conservation law for a non-relativistic matter-dominated universe, $3A = 8\pi G\rho a^3$.

The two metrics are matched on the vacuole boundary under the matching condition

$$r_{\text{Schü}}(T) = a(t) \sinh \chi_{\text{Schü}}, \quad (5)$$

where $\sin \chi_{\text{Schü}} = (2GM/A)^{1/3}$, using the fact that M is related to ρ by $3M = 4\pi r_{\text{Schü}}^3 \rho$.

Following the same treatment outlined in [4, 25–27], the Jacobian of the transformation from the Schwarzschild to the Friedmann coordinates coordinates, $(T, r) \rightarrow (t, \chi)$, on the vacuole reads

$$J = \begin{pmatrix} \cosh \chi_{\text{Schü}} & -\frac{f(a) \sinh \chi_{\text{Schü}}}{B_{\text{Schü}}} \\ -\frac{f(a) \sinh \chi_{\text{Schü}}}{a} & \frac{\cosh \chi_{\text{Schü}}}{a B_{\text{Schü}}} \end{pmatrix}, \quad (6)$$

from which one can deduce a relation allowing to pass from the Schwarzschild time to the Friedmann time and vice versa,

$$dT = \cosh \chi_{\text{Schü}} \frac{dt}{B_{\text{Schü}}(t)}, \quad (7)$$

with $B_{\text{Schü}} = B(r_{\text{Schü}})$.

III. LIGHT BENDING AND TIME DELAY

We consider two photons emitted from a source S at different times t_S and t'_S . These photons reach the boundary of the vacuole at $t_{\text{SchüS}}$ and $t'_{\text{SchüS}}$, traverse the vacuole, and exit on the opposite side at $t_{\text{SchüE}}$ and $t'_{\text{SchüE}}$. Both photons ultimately arrive simultaneously at Earth E at $t_E = t'_E$, as depicted in Fig. 1. This synchronization is motivated by the well-known observational conditions on Earth, which allow to express the time delay between the two photons as $\Delta t = t'_S - t_S$. This implies a backward integration in time. Let α and α' denote the angles that the photons make upon receipt on Earth, and r_P and r'_P the minimum approach distances (perilens) where they get deflected by a lens L .

The Earth–lens and Earth–source comoving distances, denoted by $\chi_L = \chi(z_L)$ and $\chi_S = \chi(z_S)$ are calculated from the radial geodesic equation for given redshifts z_L and z_S ,

$$\chi(z) = \int_{\frac{a_0}{1+z}}^{a_0} \frac{da}{af(a)}. \quad (8)$$

To obtain (8), I use the cosmological redshift relation $1+z = a_0/a$, where $a_0 = a(t=0)$ is the current scale factor at Earth. The Earth–Source distance χ_{LS} is approximated by

$$\chi_{LS} \simeq \chi_S - \chi_L, \quad (9)$$

due to the small source angular position φ_S .

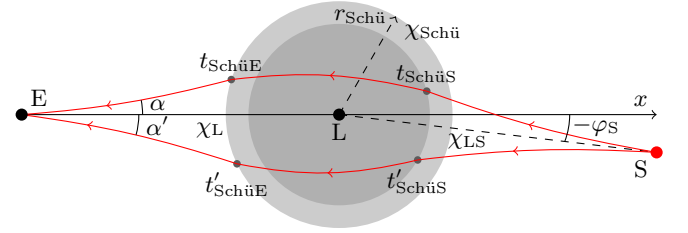


FIG. 1. Two photons emitted by a source S , bent inside the SdS vacuole by a lens L and finally received at Earth E . Outside the vacuole the trajectories diverge due to the pseudo-spherical geometry of negative curvature.

A. Integrating null geodesic equations between Earth and vacuole

Due to spherical symmetry, photon trajectories are confined to a plane, commonly chosen to be equatorial $\theta = \pi/2$. Consequently, only the t and φ components of the FLRW null geodesic equations are needed, which are

$$\ddot{t} + a\dot{a}(\dot{\chi}^2 + \sinh^2\chi\dot{\varphi}^2) = 0, \quad (10)$$

$$\frac{1}{2}\ddot{\varphi} + \frac{\dot{a}}{a} + \frac{\dot{\chi}}{\tanh\chi} = 0, \quad (11)$$

where $\dot{} = d/d\tau$, with τ an affine parameter distinct from the proper time. The upper photon would arrive at Earth with final conditions ($\tau = 0$) $t = 0$, $\chi = \chi_L$, $\varphi = \pi$, $\dot{t} = 1$, $\dot{\chi} = \cos \beta/a_0$, and $\dot{\varphi} = \sin \beta/a_0$, where we have used the fact that the physical angle α coincides with the coordinate angle, i.e., $\tan \alpha = |r_{\text{ED}} d\varphi(r_{\text{E}})/dr| = |\tanh \chi_L d\varphi(\chi_L)/d\chi|$. Then, a straightforward integration of Eqs. (10) and (11) yields

$$\dot{t} = \frac{a_0}{a(t)}, \quad \dot{\varphi} = \frac{a_0 \sinh \chi_{\text{PE}}}{a^2 \sinh^2 \chi}, \quad (12)$$

$$\varphi = \pi - \arcsin \frac{\tanh \chi_{\text{PE}}}{\tanh \chi} + \beta, \quad (13)$$

from which a relation between the variables χ and a can be derived,

$$\frac{da}{af(a)} = \frac{d\chi}{\sqrt{1 - \chi_{\text{PE}}^2 / \sinh^2 \chi}}, \quad (14)$$

where χ_{PE} and β are constants defined by $\sinh \chi_{\text{PE}} = \sinh \chi_L \sin \beta$ and $\sin \beta = \cosh \chi_L \tan \alpha$. The integration of the right-hand side of Eq. (14) can be analytically carried out leading to

$$\int_{a_{\text{SchüE}}}^{a_0} \frac{da}{af(a)} = \text{arccosh} \frac{\cosh \chi_L}{\cosh \chi_{\text{PE}}} - \text{arccosh} \frac{\cosh \chi_{\text{Schü}}}{\cosh \chi_{\text{PE}}}, \quad (15)$$

from which the value of $a_{\text{SchüE}} = a(t_{\text{SchüE}})$ is calculated by numerical integration. The corresponding value of $t_{\text{SchüE}}$ at which the upper photon emerges from the vacuole is then calculated by numerical integration of the Friedmann equation (4), i.e.,

$$t_{\text{SchüE}} = \int_{a_0}^{a_{\text{SchüE}}} \frac{da}{f(a)}. \quad (16)$$

Similar formulas apply in the case of the lower photon, with π replaced by $-\pi$ and α replaced by $-\alpha'$ regarding the Earth position.

However, one can proceed differently and calculate $t'_{\text{SchüE}}$, at which the lower photon emerges from the vacuole, in terms of $t_{\text{SchüE}}$ through an approximate formula. Subtracting the right and the left-hand sides of Eq. (15) from the ones which correspond to the lower photon, then approximating in the limit of small α and α' , one gets

$$\int_{t_{\text{SchüE}}}^{t'_{\text{SchüE}}} \frac{dt}{a(t)} \simeq \frac{1}{2} (\coth \chi_{\text{Schü}} - \coth \chi_L) \sinh^2 \chi_L \times \cosh^2 \chi_L (\alpha^2 - \alpha'^2). \quad (17)$$

Now, to approximate the left-hand side of Eq. (17), one can use the fact that $a(t)$ vary appreciably only on cosmological time intervals. The final result is

$$\Delta t_{\text{SchüE}} \simeq \frac{1}{8} a_{\text{SchüE}} (\coth \chi_{\text{Schü}} - \coth \chi_L) \sinh^2 (2\chi_L) \times (\alpha^2 - \alpha'^2). \quad (18)$$

where we have put $\Delta t_{\text{SchüE}} = t'_{\text{SchüE}} - t_{\text{SchüE}}$.

B. Integrating null geodesic equations inside the vacuole

In this region described by the SdS metric, the main task is to determine the scale factors $a_{\text{SchüS}}$ and $a'_{\text{SchüS}}$ and their corresponding times $t_{\text{SchüS}}$ and $t'_{\text{SchüS}}$, at which the upper and lower photons enter the vacuole. This is achieved by integrating geodesic equations backward from the known final conditions at the exit points from the vacuole.

The time required for the upper photon to traverse the vacuole is obtained by integration of Eq. (7),

$$T_{\text{SchüE}} - T_{\text{SchüS}} = \cosh \chi_{\text{Schü}} \int_{a_{\text{SchüS}}}^{a_{\text{SchüE}}} \frac{da}{B_{\text{Schü}}(a)f(a)}, \quad (19)$$

using the Friedmann equation (4). Another expression for this travel time can be obtained by making use of the well known equation

$$dT = \pm \frac{dr}{v(r)}, \quad v(r) = B(r) \sqrt{1 - J^2 \frac{B(r)}{r^2}}, \quad (20)$$

which follows directly from the first and second partially integrated SdS null geodesic equations, i.e.,

$$\dot{T} = \frac{1}{B(r)}, \quad \dot{r} = \pm \sqrt{1 - J^2 \frac{B(r)}{r^2}}, \quad \dot{\varphi} = \frac{J}{r^2}, \quad (21)$$

where J is a constant of motion defined by $J = r_{\text{P}}/\sqrt{B(r_{\text{P}})}$ with r_{P} the perilens given approximately by [25] $r_{\text{P}} \simeq r_{\text{SchüE}} \sin \gamma_{\text{SdS}} - GM$ with $\tan \gamma_{\text{SdS}} = |r_{\text{SchüE}} d\varphi(r_{\text{SchüE}})/dr|$ calculated using the inverse Jacobian of (6) and $r_{\text{SchüE}} = a_{\text{SchüE}} \sinh \chi_{\text{Schü}}$. The result is obtained by integrating Eq. (21), i.e.,

$$T_{\text{SchüE}} - T_{\text{SchüS}} = \left(\int_{r_{\text{P}}}^{r_{\text{SchüE}}} + \int_{r_{\text{P}}}^{r_{\text{SchüS}}} \right) \frac{dr}{v(r)}, \quad (22)$$

using the fact that r decreases over $[r_{\text{SchüS}}, r_{\text{P}}]$ while it increases over $[r_{\text{P}}, r_{\text{SchüE}}]$. Equating the two right sides of Eqs. (19) and (22), one obtains

$$\left(\int_{r_{\text{P}}}^{r_{\text{SchüE}}} + \int_{r_{\text{P}}}^{r_{\text{SchüS}}} \right) \frac{dr}{v(r)} = \int_{a_{\text{SchüS}}}^{a_{\text{SchüE}}} \frac{da}{B_{\text{Schü}}(a)f(a)} \times \cosh \chi_{\text{Schü}}, \quad (23)$$

which enables us to obtain $a_{\text{SchüS}}$ by numerical integration, with $r_{\text{SchüS}} = a_{\text{SchüS}} \sinh \chi_{\text{Schü}}$. Then one has to integrate numerically the Friedmann equation (4) to obtain $t_{\text{SchüS}}$, i.e.,

$$t_{\text{SchüS}} = \int_{a_0}^{a_{\text{SchüS}}} \frac{da}{f(a)}. \quad (24)$$

Similar formulas are applied for the lower photon leading to the calculation of the scale factor $a'_{\text{SchüS}}$ and $t'_{\text{SchüS}}$. This also can be determined by difference with $t_{\text{SchüS}}$ via an approximate analytical expression. Subtracting the

right and the left-hand side of Eq. (19) from the ones which correspond to the lower photon, and taking into account that $B_{\text{Schü}}$ is only significant on cosmological timescales, one gets

$$\Delta T_{\text{SchüE}} - \Delta T_{\text{SchüS}} \simeq \left(\frac{\Delta t_{\text{SchüE}}}{B_{\text{SchüE}}} - \frac{\Delta t_{\text{SchüS}}}{B_{\text{SchüS}}} \right) \cosh \chi_{\text{Schü}}, \quad (25)$$

with $\Delta T_{\text{SchüE}} = T'_{\text{SchüE}} - T_{\text{SchüE}}$, $\Delta T_{\text{SchüS}} = T'_{\text{SchüS}} - T_{\text{SchüS}}$, $\Delta t_{\text{SchüS}} = t'_{\text{SchüS}} - t_{\text{SchüS}}$, $B_{\text{SchüE}} = B_{\text{Schü}}(t_{\text{SchüE}})$ and $B_{\text{SchüS}} = B_{\text{Schü}}(t_{\text{SchüS}})$. This expresses the difference in the travel times between both photons inside the vacuole, which can be otherwise obtained by the use of Eq. (20), i.e.,

$$\Delta T_{\text{SchüE}} - \Delta T_{\text{SchüS}} = \left(\int_{r_{\text{SchüE}}}^{r'_{\text{SchüE}}} + \int_{r_{\text{SchüS}}}^{r'_{\text{SchüS}}} \right) \frac{dr}{v(r)} - \Delta T_{\text{SdS}}, \quad (26)$$

where we have divided the integrals to produce the following expression

$$\Delta T_{\text{SdS}} = \left(\int_{r_{\text{P}}}^{r_{\text{SchüE}}} + \int_{r_{\text{P}}}^{r_{\text{SchüS}}} \right) \frac{dr}{v(r)} - \left(\int_{r'_{\text{P}}}^{r_{\text{SchüE}}} + \int_{r'_{\text{P}}}^{r_{\text{SchüS}}} \right) \frac{dr}{v'(r)}. \quad (27)$$

This can be directly compared to an expression previ-

ously used in the calculation of the time delay within the framework of the SdS solution [28], i.e.,

$$\begin{aligned} \Delta T_{\text{SdS}} \simeq & \frac{1}{2} (r_{\text{P}}'^2 - r_{\text{P}}^2) \left(\frac{1}{r_{\text{SchüE}}} + \frac{1}{r_{\text{SchüS}}} \right) \\ & + 4GM \ln \frac{r_{\text{P}}'}{r_{\text{P}}} - \frac{3}{2} G^2 M^2 \left(\frac{1}{r_{\text{P}}^2} - \frac{1}{r_{\text{P}}'^2} \right) \sqrt{\frac{3}{\Lambda}} \\ & \times \left(\operatorname{arctanh} \sqrt{\frac{\Lambda}{3} r_{\text{SchüE}}^2} + \operatorname{arctanh} \sqrt{\frac{\Lambda}{3} r_{\text{SchüS}}^2} \right). \end{aligned} \quad (28)$$

Additionally, given that the lengths and timescales under consideration are shorter than cosmological scales, the last term on the right-hand side of Eq. (26) can be approximated as

$$\left(\int_{r_{\text{SchüE}}}^{r'_{\text{SchüE}}} + \int_{r_{\text{SchüS}}}^{r'_{\text{SchüS}}} \right) \frac{dr}{v(r)} \simeq \sinh \chi_{\text{Schü}} \left(f_{\text{SchüE}} \frac{\Delta t_{\text{SchüE}}}{v_{\text{SchüE}}} + f_{\text{SchüS}} \frac{\Delta t_{\text{SchüS}}}{v_{\text{SchüS}}} \right), \quad (29)$$

using the matching condition (5) as well as the Friedmann equation (4), with $v_{\text{SchüE}} = f(r_{\text{SchüE}})$, $v_{\text{SchüS}} = v(r_{\text{SchüS}})$, $f_{\text{SchüE}} = f(a_{\text{SchüE}})$ and $f_{\text{SchüS}} = f(a_{\text{SchüS}})$. Replacing (29) together with (28) into Eq. (26) and equating its right-hand side with the one of Eq. (25), we finally arrive at

$$\Delta t_{\text{SchüS}} \simeq \frac{\Delta T_{\text{SdS}} + \left(\frac{\cosh \chi_{\text{Schü}}}{B_{\text{SchüE}}} - \frac{f_{\text{SchüE}} \sinh \chi_{\text{Schü}}}{v_{\text{SchüE}}} \right) \Delta t_{\text{SchüE}}}{\frac{\cosh \chi_{\text{Schü}}}{B_{\text{SchüS}}} + \frac{f_{\text{SchüS}} \sinh \chi_{\text{Schü}}}{v_{\text{SchüS}}}}. \quad (30)$$

The determination of $t_{\text{SchüS}}$ allows us to compute the polar angle $\varphi_{\text{SchüS}}$ at which the photon arrives on the boundary of the vacuole, a quantity required for the subsequent analysis in Subsec. III C. This is achieved by employing the well-known equation

$$d\varphi = \pm \frac{dr}{u(r)}, \quad u(r) = r \sqrt{\frac{r^2}{J^2} - B(r)}, \quad (31)$$

which follow immediately from the second and third partially integrated SdS null geodesic equations in (21). Integrating Eq. (31) yields

$$\varphi_{\text{SchüE}} - \varphi_{\text{SchüS}} = \left(\int_{r_{\text{P}}}^{r_{\text{SchüE}}} + \int_{r_{\text{P}}}^{r_{\text{SchüS}}} \right) \frac{dr}{v(r)}, \quad (32)$$

where we account for the fact that φ increases both as the photon approaches the lens and as it recedes from it. The right hand side of Eq. (32) can be evaluated analytically

to leading order in the ratio of Schwarzschild radius to perilens, $2GM/r_{\text{P}}$, resulting in

$$\begin{aligned} \varphi_{\text{SchüS}} \simeq & \varphi_{\text{SchüE}} - \pi + \arcsin \frac{r_{\text{P}}}{r_{\text{SchüE}}} + \arcsin \frac{r_{\text{P}}}{r_{\text{SchüS}}} \\ & - \frac{GM}{r_{\text{P}}} \left(\sqrt{1 - \frac{r_{\text{P}}^2}{r_{\text{SchüE}}^2}} + \sqrt{1 - \frac{r_{\text{P}}^2}{r_{\text{SchüS}}^2}} \right. \\ & \left. + \sqrt{\frac{r_{\text{SchüE}} - r_{\text{P}}}{r_{\text{SchüE}} + r_{\text{P}}}} + \sqrt{\frac{r_{\text{SchüS}} - r_{\text{P}}}{r_{\text{SchüS}} + r_{\text{P}}}} \right), \end{aligned} \quad (33)$$

with $\varphi_{\text{SchüE}} = \varphi(t_{\text{SchüE}}) = \varphi(\chi_{\text{Schü}})$ given by Eq. (13).

C. Integrating null geodesic equations between vacuole and source

The motion of photons in this region is governed by the same FLRW geodesic equations, (10) and (11), treated

in Subsec. III A. One must integrate them in order to obtain the scale factor a_S and its corresponding emission time t_S of the upper photon at the source S, taking into account the final conditions at the entry into the vacuole, i.e., $t = t_{\text{Sch\"us}}$, $\chi = \chi_{\text{Sch\"u}}$, $\varphi = \varphi_{\text{Sch\"us}}$, $\dot{t} = \dot{t}_{\text{Sch\"us}}$, $\dot{\chi} = \dot{\chi}_{\text{Sch\"us}}$, and $\dot{\varphi} = \dot{\varphi}_{\text{Sch\"us}}$, which are calculated using the Jacobian (6). We obtain

$$\dot{t} = \frac{E}{a(t)}, \quad \dot{\varphi} = \frac{J}{a^2 \sinh^2 \chi}, \quad (34)$$

$$\varphi = \varphi_{\text{Sch\"us}} + \arcsin \frac{\tanh \chi_{\text{PS}}}{\tanh \chi} - \gamma, \quad (35)$$

where E , χ_{PS} , and γ are constants related to each other by $E = a_{\text{Sch\"us}} \dot{t}_{\text{Sch\"us}}$, $\sinh \chi_{\text{PS}} = J/E$, and $\sin \gamma = \tanh \chi_{\text{PS}} / \tanh \chi_{\text{Sch\"u}}$. Hence, the source angular position φ_S corresponding to the comoving distance χ_{LS} (9) is calculated using Eq. (35), i.e.,

$$-\varphi_S = -\varphi_{\text{Sch\"us}} - \arcsin \frac{\tanh \chi_{\text{PS}}}{\tanh \chi_{\text{LS}}} + \gamma, \quad (36)$$

where $\varphi_{\text{Sch\"us}}$ is given by (33).

In a similar manner to the upper photon, analogous formulas are obtained for the lower photon, with the only difference being that the constant J' differs by a minus sign, $J' = -r'_P / \sqrt{B(r'_P)}$ with $r'_P \simeq r'_{\text{Sch\"uE}} \sin \gamma'_{\text{SdS}} - GM$ and $\tan \gamma'_{\text{SdS}} = |r'_{\text{Sch\"uE}} d\varphi(r'_{\text{Sch\"uE}})/dr|$. The expression of the source angular position φ'_S , which corresponds to the same comoving distance χ_{LS} , is then

$$-\varphi'_S = -\varphi'_{\text{Sch\"us}} + \arcsin \frac{\tanh \chi'_{\text{PS}}}{\tanh \chi_{\text{LS}}} - \gamma', \quad (37)$$

where χ'_{PS} is a constant related to J' and the constant of motion $E' = a'_{\text{Sch\"us}} \dot{t}'_{\text{Sch\"us}}$ by $\sinh \chi'_{\text{PS}} = J'/E'$, and $\sin \gamma' = \tanh \chi'_{\text{PS}} / \tanh \chi_{\text{Sch\"u}}$.

These angles φ_S and φ'_S must coincide, as both photons originate from the same source. Among all the parameters involved, adjusting the lens mass appears to be the only effective means to equate them. Once the accurate mass is determined, the calculation of the time delay can proceed.

As before, an equation similar to (14) linking χ to a can be derived from Eqs. (34) and (35),

$$\frac{da}{af(a)} = - \frac{d\chi}{\sqrt{1 - \sinh^2 \chi_{\text{PS}} / \sinh^2 \chi}}, \quad (38)$$

where the minus sign reflects a decreasing function over time in this region. Then integrating between χ_{LS} and $\chi_{\text{Sch\"u}}$ leads to

$$\int_{a_S}^{a_{\text{Sch\"us}}} \frac{da}{af(a)} = \text{arccosh} \frac{\cosh \chi_{\text{LS}}}{\cosh \chi_{\text{PS}}} - \text{arccosh} \frac{\cosh \chi_{\text{Sch\"u}}}{\cosh \chi_{\text{PS}}}, \quad (39)$$

which can be numerically solved to calculate a_S . Then, t_S is calculated through the Friedmann equation as

$$t_S = \int_{a_0}^{a_S} \frac{da}{f(a)}. \quad (40)$$

Similar formulas are applied regarding the lower photon, replacing $a_{\text{Sch\"us}}$ by $a'_{\text{Sch\"us}}$ and χ_{PS} by χ'_{PS} .

Now, let us proceed differently to calculate the time delay via an approximate expression. Subtracting the two sides of (39) from the ones of the lower photon, and approximating in the limit of small $\varphi_{\text{Sch\"us}} - \varphi_S$ and $|\varphi'_{\text{Sch\"us}} - \varphi_S|$ ($\sim 10^{-4}$), one gets

$$\left(\int_{t_{\text{Sch\"us}}}^{t'_{\text{Sch\"us}}} - \int_{t_S}^{t'_S} \right) \frac{dt}{a(t)} \simeq \frac{1}{2} \frac{(\varphi'_{\text{Sch\"us}} - \varphi_S)^2 - (\varphi_{\text{Sch\"us}} - \varphi_S)^2}{\coth \chi_{\text{Sch\"u}} - \coth \chi_{\text{LS}}}. \quad (41)$$

Approximating the left-hand side of (41) using the fact that the scale factor $a(t)$ varies noticeably only over cosmological timescales, one obtains finally the time delay formula

$$\Delta t \simeq a_S \left[\frac{\Delta t_{\text{Sch\"us}}}{a_{\text{Sch\"us}}} - \frac{1}{2} \frac{(\varphi'_{\text{Sch\"us}} - \varphi_S)^2 - (\varphi_{\text{Sch\"us}} - \varphi_S)^2}{\coth \chi_{\text{Sch\"u}} - \coth \chi_{\text{LS}}} \right]. \quad (42)$$

IV. THE LENSED QUASAR SDSS J1004+4112

The results are now applied to the lensed quasar SDSS J1004+4112 discovered by Inada et al. [29]. This system clearly exhibits a strong gravitational lensing caused by a galaxy cluster at a redshift $z_L = 0.68$, producing five images of a background quasar at redshift $z_S = 1.734$. The lens is assumed to be symmetric, despite the fact that the presence of five images shows it is not. Here, we only consider the very large angular separation of about

15 arcseconds between images C and D, with $\alpha = 5'' \pm 10\%$ (D) and $\alpha' = 10'' \pm 10\%$ (C).

For numerical convenience, we use a system of astro-units introduced by Sch\"ucker in Ref. [25], in which time, distances, and masses are measured in astroseconds (as), astrometers (am) and astrograms (ag), respectively, as

TABLE I. Galaxy cluster mass M , position angle $-\varphi_S$, and time delay Δt for the observed image pair (D,C) of the lensed quasar SDSS J1004+4112 in hyperbolic Einstein-Straus-de Sitter spacetime ($k = -1$). The cosmic scale factor is fixed in the value $a_0 = 5 \text{ am}$ ($\Omega_{k0} = -0.04$).

$(\Lambda, \alpha, \alpha')$	$M[10^{13} M_\odot]$	$-\varphi_S[']$	$\Delta t[\text{yr}]$
(+, +, +)	2.208632	9.89304	12.1077
(+, +, ± 0)	2.007476	8.10108	9.40788
(+, +, -)	1.806348	6.30938	6.92009
(+, ± 0 , +)	2.008189	10.7857	12.6577
(+, ± 0 , ± 0)	1.8253007	8.99358	10.0078
(+, ± 0 , -)	1.6424348	7.20165	7.56259
(+, -, +)	1.8077	11.6787	13.0953
(+, -, ± 0)	1.6430808	9.88629	10.5029
(+, -, -)	1.478481	8.09413	8.10762
(± 0 , +, +)	2.24554	11.0019	12.0502
(± 0 , +, ± 0)	2.041158	9.00591	9.3712
(± 0 , +, -)	1.836798	7.01012	6.89681
(± 0 , ± 0 , +)	2.041581	11.9976	12.5832
(± 0 , ± 0 , ± 0)	1.855775	10.0015	9.96047
(± 0 , ± 0 , -)	1.6699799	8.00555	7.53374
(± 0 , -, +)	1.8375975	12.9934	12.9971
(± 0 , -, ± 0)	1.670366	10.9972	10.4397
(± 0 , -, -)	1.503141	9.0011	8.06935
(-, +, +)	2.220931	11.6782	11.7829
(-, +, ± 0)	2.01884	9.55814	9.16816
(-, +, -)	1.8167686	7.43828	6.74997
(-, ± 0 , +)	2.019142	12.7363	12.2957
(-, ± 0 , ± 0)	1.835426	10.6162	9.7396
(-, ± 0 , -)	1.65171415	8.49622	7.37091
(-, -, +)	1.817342	13.7945	12.6882
(-, -, ± 0)	1.625673	12.1218	9.96458
(-, -, -)	1.4866455	9.55423	7.89049

follows:

$$1 \text{ as} = 4.34 \times 10^{17} \text{ s} = 13.8 \text{ Gyr}, \quad (43)$$

$$1 \text{ am} = 1.30 \times 10^{26} \text{ m} = 4221 \text{ Mpc}, \quad (44)$$

$$1 \text{ ag} = 6.99 \times 10^{51} \text{ kg} = 3.52 \times 10^{21} M_\odot. \quad (45)$$

In this astro-unit system, the fundamental constants take the values: $c = 1 \text{ am as}^{-1}$, $8\pi G = 1 \text{ am}^3 \text{ as}^{-2} \text{ ag}^{-1}$, and $H_0 = 1 \text{ as}^{-1}$ ($= 71 \text{ km s}^{-1} \text{ Mpc}^{-1}$), with H_0 the Hubble constant involved in the Hubble law $da/dt = H_0 a(t)$. Substituting this into the Friedmann equation (4) yields $A = \rho_0 a_0^3/3$ with the current dust density $\rho_0 = 3 - \Lambda + 3\Omega_{k0}$ and current curvature density $\Omega_{k0} = k/a_0^2 = -1/a_0^2$. We use throughout this work the same cosmological constant adopted in [25–27], $\Lambda = 1.36 \times 10^{-52} \text{ m}^{-2} = 0.77 \times 3 \text{ am}^{-2}$, with an accuracy of 20%. To guarantee a definite positive dust density $\rho_0 > 0$, the current scale factor a_0 must satisfy $a_0 > 1/\sqrt{1 - \Lambda/3} \simeq 2.08514 \text{ am}$. This lower bound translates into a constraint on the current curvature density, $|\Omega_{k0}| < 0.23$, ensuring that the cosmological parameters are physically consistent with the Friedmann equation in the adopted unit system. The comoving distances χ_L and χ_S , and χ_{LS} are calculated from (8) and (9).

To quantify the influence of Λ on light bending, Table I

TABLE II. Variation of the galaxy cluster mass M , the position angle $-\varphi_S$, and the time delay Δt versus the current cosmic scale factor a_0 for the observed image pair (D,C) of the lensed quasar SDSS J1004+4112 in hyperbolic Einstein-Straus-de Sitter spacetime ($k = -1$). The cosmological constant Λ as well as the angles α and α' are fixed in their central values.

$a_0[\text{am}]$	$M[10^{13} M_\odot]$	$-\varphi_S[']$	$\Delta t[\text{yr}]$
2.1	2.016437	10.0961	11.301
2.2	1.99955	10.0913	11.1473
2.3	1.984515	10.0854	11.01
2.4	1.971193	10.0792	10.8918
2.5	1.9593693	10.0731	10.7893
2.6	1.948855	10.0673	10.6999
2.7	1.939484	10.0617	10.6215
2.8	1.931099	10.0565	10.5522
2.9	1.923578	10.0517	10.4907
3.0	1.916802	10.0472	10.4359
3.2	1.905132	10.0392	10.3425
3.4	1.895497	10.0322	10.2663
3.6	1.88745	10.0263	10.2034
3.8	1.880665	10.0212	10.1507
4.0	1.874885	10.0167	10.1061
4.5	1.863721	10.0079	10.0207
5.0	1.855775	10.0015	9.96047
6.0	1.845481	9.99297	9.88309
7.0	1.839308	9.98776	9.83703
8.0	1.835316	9.98435	9.80736
9.0	1.832585	9.98200	9.78712
10.0	1.8306345	9.98031	9.7727
11.0	1.829193	9.97906	9.76206
12.0	1.828098	9.97811	9.75398
13.0	1.8272465	9.97737	9.7477
14.0	1.8265714	9.97678	9.74273
15.0	1.8260268	9.9763	9.73872
16.0	1.825581	9.97591	9.73544
17.0	1.8252119	9.97559	9.73272
18.0	1.8249025	9.97532	9.73044
19.0	1.8246409	9.97509	9.72852
20.0	1.824417	9.97489	9.72688
21.0	1.824225	9.97472	9.72546
22.0	1.8240586	9.97457	9.72424
23.0	1.8239134	9.97445	9.72317
24.0	1.82378576	9.97433	9.72224
25.0	1.8236734	9.97424	9.72141
26.0	1.823574	9.97415	9.72068
27.0	1.823485	9.97407	9.72002
28.0	1.823405	9.974	9.71944
29.0	1.8233336	9.97394	9.71891
30.0	1.823269	9.97388	9.71844
31.0	1.823211	9.97383	9.71801
32.0	1.823158	9.97378	9.71762
33.0	1.82311	9.97374	9.71727
34.0	1.823066	9.9737	9.71695
35.0	1.8230256	9.97367	9.71665
36.0	1.8229884	9.97363	9.71638
37.0	1.8229545	9.9736	9.71613
38.0	1.8229234	9.97358	9.7159
39.0	1.822894	9.97355	9.71569
40.0	1.8228676	9.97353	9.71549

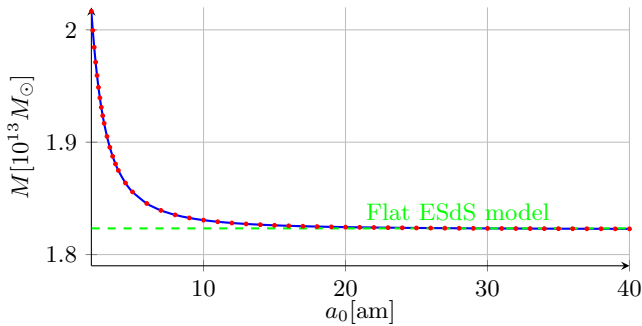


FIG. 2. Evolution of galaxy cluster mass M with current cosmic scale factor a_0 in hyperbolic Einstein-Straus-de Sitter model.

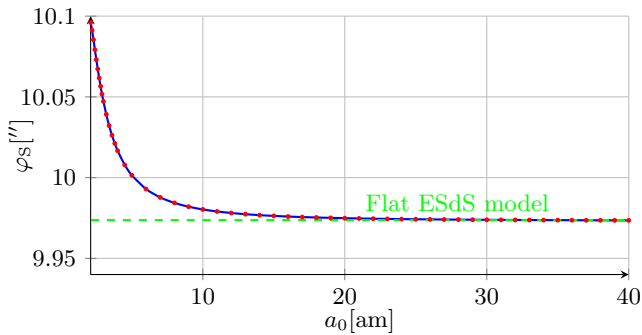


FIG. 3. Evolution of deflection angle $-\varphi_S$ with current cosmic scale factor a_0 in hyperbolic Einstein-Straus-de Sitter model.

has been made to present the adjusted mass and the deflection angle φ_S ($= \varphi'_S$) for the maximal $+$, central ± 0 , and minimal $-$ values of Λ as well as the angles α and α' , employing a fixed current scale factor at $a_0 = 5$ am, corresponding to $\Omega_{k0} = -0.04$). For each configuration, the time delay of the photon α relative to the photon α' is computed. Note that neither Λ nor a_0 adjustments reconcile the φ_S angles.

The results presented in Table I can be succinctly summarized by the following parameter ranges: $1.48 \times 10^{13} M_\odot \leq M \leq 2.25 \times 10^{13} M_\odot$, $6.31'' \leq -\varphi_S \leq 13.79''$,

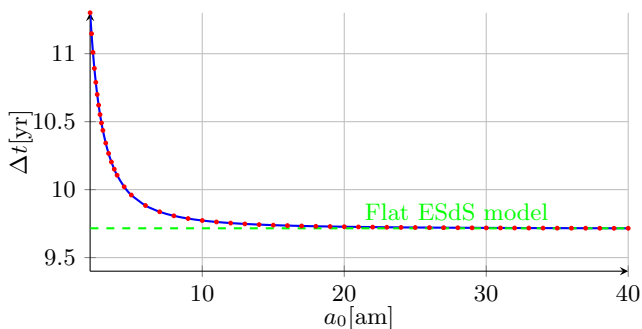


FIG. 4. Evolution of time delay Δt with current cosmic scale factor a_0 in hyperbolic Einstein-Straus-de Sitter model.

and $6.75 \text{ yr} \leq \Delta t \leq 13.10 \text{ yr}$. The galaxy cluster mass is underestimated compared to observations [29, 30], due to the spherical lens assumption. The predicted time delays are comparable with the observational lower bound $\Delta t_{\text{CD}} > 7.7 \text{ yr}$ from Fohlmeister [31] as well as the upper bound $\Delta t_{\text{CD}} \lesssim 10.14 \text{ yr}$ from Kawano and Oguri [32], who employed a non-spherical lens model.

An analysis of Table I reveals several important quantitative effects of varying the cosmological constant on gravitational lensing by a galaxy cluster. A 20% increase in the cosmological constant Λ reduces the deflection angle φ_S by approximately 9.02%, while the galaxy cluster mass changes by only 0.28%. For comparison, this reduction slightly exceeds the effect observed with $\Omega_{k0} = 0.04$ in the positively curved case [27], where the deflection angle is diminished by 8.03%. We thus conclude that a positive Λ weakens light deflection in agreement with the statement by Rindler and Ishak [5].

Table II shows how the mass, deflection angle, and time delay vary depending on different values of a_0 over the range $[2.1 \text{ am}, 40 \text{ am}]$, while holding Λ , α and α' fixed at their central values. To better visualize this dependence, we present interpolated plots in Figs. 2, 3, and 4 for the data sets (M, a_0) , $(-\varphi_S, a_0)$, and $(\Delta t, a_0)$, respectively. Contrary to the flat ESdS model, where the lensing observables remain the same regardless of the current scale factor value, the results obtained in the hyperbolic ESdS model indicate that the mass, deflection angle, and time delay increase as a_0 becomes more smaller than a limiting value close to 20 am (corresponding to a current curvature density $\Omega_{k0} \simeq -0.0025$), while above this limit, the results become independent of a_0 and compatible with the flat case [26]. The same applies for all possible values of Λ , α and α' within their error bars. Specifically, for a negative curvature density $\Omega_{k0} = -0.15$, the light bending increases slightly by about 0.94%, whereas time delay increases significantly by about 10.17%. Comparing to the positively curved case [27], with a positive curvature density $\Omega_{k0} = 0.15$, the light bending and time delay decrease by about 0.66% and 8.91% respectively, which are slightly less than the effect produced in the negatively curved case. It is worth noting that even with this relatively large negative curvature, which tends to increase lensing observables, varying the value of the cosmological constant within its error margin results in a reduction of the deflection angle by approximately 6.72%. This highlights that Λ effect on light bending does not vanish even when the Universe has substantial negative curvature; rather, it still acts to reduce light bending in the same direction as in flat or positively curved universes.

V. CONCLUSION

This work extends gravitational lensing analysis to the negatively curved Einstein-Straus-de Sitter model, providing distinct predictions for light deflection and time delay compared to the flat and positively curved mod-

els. The model uses a Swiss cheese approach, whereby a static SdS vacuole is matched to an expanding FLRW universe with negative spatial curvature $k = -1$.

Throughout the computation of light deflection and time delay, I employed a hybrid analytical-numerical integration of differential equations in each region to address the non-flat case.

An application to the lensed quasar SDSS J1004+4112 permits to quantify the subtle interplay between the spatial curvature and the cosmological constant in gravitational lensing phenomena. The results demonstrate that negative curvature enhances gravitational lensing effects, leading to larger observable quantities, while a positive Λ opposes this enhancement by reducing the deflection angle, as asserted by Rindler and Ishak. The study, based on varying the current scale factor a_0 , reveals a critical threshold of $a_0 \simeq 2.6 \times 10^{27}$ m, below which lensing observables increase markedly, linked to a current curvature density $\Omega_{k0} \lesssim -0.0025$. Specifically, for a negative curvature density $\Omega_{k0} = -0.15$, the light bending increases slightly by about 0.94%, whereas time delay increases significantly by about 10.17%. This provides a unique signature for the negatively curved universe, distinct from the positively curved case. Beyond this threshold, results match the flat ESdS model. Such a sensitivity to the curvature parameter means that precise lensing observations could, in principle, help discriminate between

open, flat, and closed universes. The study reveals that the effect of Λ on lensing does persist even in scenarios dominated by significant negative curvature and should be included in precise lensing analyses, especially when aiming to constrain cosmological parameters using strong lensing systems. Note that a positive Λ reduces light deflection because its repulsive effect counteracts spacetime curvature induced by mass.

Nevertheless, our analysis is subject to certain limitations. The assumption of a spherically symmetric lens and the use of the Swiss-cheese model, while physically motivated, may underestimate the complexity of real astrophysical systems. Future work should extend the present approach to include more realistic mass distributions, and to consider additional lensed systems with well-constrained observational data.

Another promising direction for future work is to incorporate the interior SdS solution, which describes the spacetime inside a spherically incompressible mass with a cosmological constant. Unlike the exterior case, the interior solution introduces a direct dependence of light deflection on Λ , leading to subtle corrections in lensing observables, as shown by Schücker [33]. Incorporating this effect would yield a more complete and accurate description of strong lensing by massive objects, and could help refine cosmological constraints through high-precision lensing measurements [34, 35].

-
- [1] A. Einstein and E. G. Straus, The influence of the expansion of space on the gravitation fields surrounding the individual star, *Rev. Mod. Phys.* **17**, 120 (1945).
 - [2] A. Einstein and E. G. Straus, Corrections and additional remarks to our paper: The influence of the expansion of space on the gravitation fields surrounding the individual stars, *Rev. Mod. Phys.* **18**, 148 (1946).
 - [3] R. Balbinot, R. Bergamini, and A. Comastri, Solution of the einstein-strauss problem with a Λ term, *Phys. Rev. D* **38**, 2415 (1988).
 - [4] M. Guenouche, Effect of the spatial curvature on light bending and time delay in a curved Einstein-Straus-de Sitter spacetime, *Phys. Rev. D* **110**, 063508 (2024).
 - [5] W. Rindler and M. Ishak, Contribution of the cosmological constant to the relativistic bending of light revisited, *Phys. Rev. D* **76**, 043006 (2007).
 - [6] M. Ishak, W. Rindler, J. Dossett, J. Moldenhauer, and C. Allison, A new independent limit on the cosmological constant/dark energy from the relativistic bending of light by galaxies and clusters of galaxies, *Mon. Not. R. Astron. Soc.* **388**, 1279 (2008).
 - [7] T. Schücker, Cosmological constant and lensing, *Gen. Relativ. Gravit.* **41**, 67 (2009).
 - [8] T. Schücker, Strong lensing with positive cosmological constant (2008), [arXiv:0805.1630](#).
 - [9] M. Sereno, Role of Λ in the cosmological lens equation, *Phys. Rev. Lett.* **102**, 021301 (2009).
 - [10] I. B. Khriplovich and A. A. Pomeransky, Does the cosmological term influence gravitational lensing?, *Int. J. Mod. Phys. D* **17**, 2255 (2008).
 - [11] M. Park, Rigorous approach to gravitational lensing, *Phys. Rev. D* **78**, 023014 (2008).
 - [12] F. Simpson, J. A. Peacock, and A. F. Heavens, On lensing by a cosmological constant, *Mon. Not. R. Astron. Soc.* **402**, 2009 (2010).
 - [13] R. Kantowski, B. Chen, and X. Dai, Gravitational lensing corrections in flat Λ CDM cosmology, *Astrophys. J.* **718**, 913 (2010).
 - [14] T. Schücker, Lensing in the Einstein-Straus solution (2010), [arXiv:1006.3234](#).
 - [15] B. Chen, R. Kantowski, and X. Dai, Gravitational lens equation for embedded lenses; magnification and ellipticity, *Phys. Rev. D* **84**, 083004 (2010).
 - [16] R. Kantowski, B. Chen, and X. Dai, Image properties of embedded lenses, *Phys. Rev. D* **86**, 083009 (2012).
 - [17] H. Arakida and M. Kasai, Effect of the cosmological constant on the bending of light and the cosmological lens equation, *Phys. Rev. D* **85**, 023006 (2012).
 - [18] R. Kantowski, B. Chen, and X. Dai, Fermat's least-time principle and the embedded transparent lens, *Phys. Rev. D* **86**, 083001 (2013).
 - [19] J. Sultana, Contribution of the cosmological constant to the bending of light in Kerr-de Sitter spacetime, *Phys. Rev. D* **88**, 042003 (2013).
 - [20] M. Heydari-Fard, M. Heydari-Fard, and H. R. Sepang, Bending of light in novel 4D Gauss-Bonnet-de Sitter black holes by the Rindler-Ishak method, *Europhys. Lett.* **133**, 50006 (2021).
 - [21] L. Hu, A. Heavens, and D. Bacon, Light bending by the cosmological constant, *J. Cosmol. Astropart. Phys.* **02**

- (2022), 009.
- [22] J. Sultana, Comment on “gravitational lensing in Weyl gravity”, *Phys. Rev. D* **108**, 108501 (2023).
 - [23] J. Sultana, Gravitational light bending in Weyl gravity and Schwarzschild–de Sitter spacetime, *Symmetry* **16**, 101 (2024).
 - [24] Y. Lu, X.-Y. Pan, M.-Y. Lai, and Q.-H. Wang, Finite-distance gravitational lensing of a global monopole in Schwarzschild-de Sitter spacetime (2025), [arXiv:2504.00777](#).
 - [25] T. Schücker, Strong lensing in the Einstein-Straus solution, *Gen. Relativ. Gravit.* **41**, 1595 (2009).
 - [26] K.-E. Boudjemaa, M. Guenouche, and S. R. Zouzou, Time delay in the Einstein-Straus solution, *Gen. Relativ. Gravit.* **43**, 1707 (2011).
 - [27] M. Guenouche and S. R. Zouzou, Deflection of light and time delay in closed Einstein-Straus solution, *Phys. Rev. D* **98**, 123508 (2018).
 - [28] T. Schücker and N. Zaimen, Cosmological constant and time delay, *Astron. Astrophys.* **484**, 103 (2008).
 - [29] N. Inada *et al.*, A gravitationally lensed quasar with quadruple images separated by 14.62 arcseconds, *Nature* **426**, 810 (2003).
 - [30] M. Oguri *et al.*, Observations and theoretical implications of the large separation lensed quasar SDSS J1004+4112, *Astrophys. J.* **605**, 78 (2004).
 - [31] J. Fohlmeister, C. S. Kochanek, E. E. Falco, C. W. Morgan, and J. Wambsganss, The rewards of patience: An 822 day time delay in the gravitational lens SDSS J1004+4112, *Astrophys. J.* **676**, 761 (2008).
 - [32] Y. Kawano and M. Oguri, Time delays for the giant quadruple lensed SDSS J1004+4112: Prospects for determining the density profile of the lensing cluster, *Publ. Astron. Soc. Jpn.* **58**, 271 (2006).
 - [33] T. Schücker, Lensing in an interior Kottler solution, *Gen. Relativ. Gravit.* **42**, 1991 (2010).
 - [34] M. Guenouche, Lensing in matched exterior and interior Kottler solution (2025), in preparation.
 - [35] M. Guenouche, Time delay in matched exterior and interior Kottler solution (2025), in preparation.